

# Progressive Steps towards Global Validated Simulation of Edge Plasma Turbulence

P. Ricci<sup>1</sup>, A. Fasoli<sup>1</sup>, I. Furno<sup>1</sup>, J. Loizu<sup>1</sup>, S. Jolliet<sup>1</sup>, F. Halpern<sup>1</sup>, A. Masetto<sup>1</sup>, B.N. Rogers<sup>2</sup> and C. Theiler<sup>1</sup>

<sup>1</sup>Ecole Polytechnique Fédérale de Lausanne (EPFL), Centre de Recherches en Physique des Plasmas Association Euratom-Confédération Suisse, CH-1015 Lausanne, Switzerland

<sup>2</sup>Department of Physics and Astronomy, Dartmouth College, Hanover NH 03755

*Corresponding Author:* paolo.ricci@epfl.ch

## Abstract:

Simulations of edge turbulence are particularly challenging due to the presence of large amplitude fluctuations and to the coupling of equilibrium and fluctuating scales. The Global Braginskii Solver (GBS) code has been developed to simulate plasma turbulence in edge-relevant conditions. We have initially studied relatively simple configurations of increasing complexity, linear magnetic configurations and the Simple Magnetized Torus. GBS has now reached the capabilities of performing non-linear self-consistent global three-dimensional simulations of the plasma dynamics in the Scrape-Off Layer (SOL). By solving the drift-reduced Braginskii equations, the code evolves self-consistently the density and heat fluxes from the core, turbulent transport, and the plasma losses to the limiter plates. This gradual approach has allowed gaining a deep understanding of turbulence, from identifying the driving instabilities to estimating the turbulence saturation amplitude. In particular, we point out the need of global simulations to correctly represent the SOL dynamics, simultaneously describing both fluctuating and equilibrium quantities. While validating edge simulations is necessary to assess the accuracy of our understanding, difficulties in experimental diagnostics and the lack of a precise validation methodology have, to date, severely limited the process. Therefore, a code validation development project has been conducted side by side with the GBS development. A methodology to carry out experiment-simulation comparison had been established and applied to quantify the level of agreement between the GBS results and the TORPEX experiment.

## 1 Introduction

In the last few years, the Global Braginskii Solver code, GBS, has been developed with the goal of simulating plasma SOL turbulence by evolving the full profiles of the various quantities with no separation between “perturbations” and “equilibrium”. These simulations can explore the self-consistent evolution and structure of the plasma profiles in the presence of (i) plasma density and heat input from the core of the fusion machine, (ii) cross-field transport produced by plasma instabilities (interchange instability or drift

waves, for example), and (iii) parallel losses at the sheaths where the magnetic field lines terminate on the walls.

In order to progressively approach the complexity of tokamak edge simulations, the GBS code was initially developed and used to simulate turbulent dynamics in basic plasma physics devices of increasing complexity [1, 2, 3, 4, 5, 6, 7, 8, 9, 10]. Featuring some of the main elements of SOL plasma dynamics, these devices offer a simple and well-diagnosed testbed to study the basic physics of plasma edge turbulence and the associated transport of heat and particles in a simplified environment. In particular, the initial GBS simulations were focused on linear devices, such as LAPD [11], and on the simple magnetized plasma torus (SMT), such as the TORPEX device [12, 13], in which a vertical magnetic field  $B_v$ , superimposed on a toroidal field  $B_\phi$ , creates helicoidal field lines with both ends terminating on the torus vessel. The first version of the code was able to follow two-dimensional plasma dynamics in the plane perpendicular to the magnetic field [1, 2, 3, 5, 8, 10], and was developed from ESEL [14, 15], a code that implements the algorithm described in Ref. [16]. The two-dimensional code was used for the simulation of ideal interchange SMT turbulence, based on the fact that in this regime  $k_\parallel = 0$ . GBS was then extended to the third dimension, in order to describe the dynamics in the direction parallel to the magnetic field, first to perform flux-tube simulations [4], reaching then the capability of performing global simulations of SMT and linear devices [6, 7, 8, 9]. As described in the present paper, GBS now allows simulations of the tokamak SOL.

Validation of edge turbulence codes is challenging because of the difficult diagnostic access in tokamak plasmas and the complexity of the interpretation of the experimental measurements. In parallel with the GBS development, a validation project of the GBS data has been carried out [3, 8]. First, we have established a rigorous framework to compare quantitatively simulations and experiments. Second, being applied to a well-diagnosed basic plasma physics experiment such as TORPEX, we have been able to compare the GBS results to experimental data in great detail.

The goal of the present paper is to present the model considered by GBS and the first results of SOL simulations. We also discuss the main results of the validation project that has been carried out within the GBS development.

## 2 The GBS system of equations

At the plasma edge, where collisionality plays a dominant role and kinetic effects such as particle trapping and wave-particle resonance are less important, fluid modelling is still an appropriate choice to perform global turbulence simulations at a computational cost that allows a wide parameter scan. We adopt the drift ordering, which is based on assuming that  $d/dt \ll \omega_{ci}$  and that turbulence is essentially aligned with the field-line,  $|\nabla_\parallel| \ll |\nabla_\perp|$ . Within the drift ordering, it is useful to split the analysis of the dynamics into the direction parallel and perpendicular to the magnetic field, by decomposing  $\mathbf{V}_\alpha = V_{\parallel\alpha} \mathbf{b} + \mathbf{v}_{\perp\alpha}$ . Using the plasma velocity evaluated within the drift ordering, it is possible to derive the equations that are solved by GBS. Within this derivation, we consider the cold ion approximation,  $T_i \ll T_e$ , neglecting  $p_i$  effects.

The model implemented in the GBS code is constituted by the continuity equation, the vorticity equation, Ampere's law, the equation for the ion and electron parallel motion, and the equation for the electron temperature:

$$\begin{aligned} \frac{\partial n}{\partial t} = & -\frac{R}{\rho_{s0}} \frac{1}{B} [\phi, n] + \frac{2n}{B} \left[ C(T_e) + \frac{T_e}{n} C(n) - C(\phi) \right] \\ & -n(\mathbf{b} \cdot \nabla) V_{\parallel e} - V_{\parallel e}(\mathbf{b} \cdot \nabla)n + \mathcal{D}_n(n) + S \end{aligned} \quad (1)$$

$$\begin{aligned} \frac{\partial \omega}{\partial t} = & -\frac{R}{\rho_{s0}} \frac{1}{B} [\phi, \omega] - V_{\parallel i}(\mathbf{b} \cdot \nabla)\omega + B^2 \left[ (\mathbf{b} \cdot \nabla)(V_{\parallel i} - V_{\parallel e}) \right. \\ & \left. + \frac{(V_{\parallel i} - V_{\parallel e})}{n} (\mathbf{b} \cdot \nabla)n \right] \\ & + 2B \left[ C(T_e) + \frac{T_e}{n} C(n) \right] + \frac{B}{3n} C(G_i) + \mathcal{D}_\omega(\omega) \end{aligned} \quad (2)$$

$$\begin{aligned} \frac{\partial V_{\parallel e}}{\partial t} + \frac{m_i \beta_e}{m_e} \frac{\partial \psi}{2 \partial t} = & -\frac{R}{\rho_{s0}} \frac{1}{B} [\phi, V_{\parallel e}] - V_{\parallel e}(\mathbf{b} \cdot \nabla)V_{\parallel e} - \frac{m_i}{m_e} \frac{2}{3} (\mathbf{b} \cdot \nabla)G_e \\ & - \frac{m_i}{m_e} \nu (V_{\parallel e} - V_{\parallel i}) + \frac{m_i}{m_e} (\mathbf{b} \cdot \nabla)\phi - \frac{m_i T_e}{nm_e} (\mathbf{b} \cdot \nabla)n \\ & - 1.71 \frac{m_i}{m_e} (\mathbf{b} \cdot \nabla)T_e + \mathcal{D}_{V_{\parallel e}}(V_{\parallel e}) \end{aligned} \quad (3)$$

$$\begin{aligned} \frac{\partial V_{\parallel i}}{\partial t} = & -\frac{R}{\rho_{s0}} \frac{1}{B} [\phi, V_{\parallel i}] - V_{\parallel i}(\mathbf{b} \cdot \nabla)V_{\parallel i} - \frac{2}{3} (\mathbf{b} \cdot \nabla)G_i \\ & - \left[ (\mathbf{b} \cdot \nabla)T_e + \frac{T_e}{n} (\mathbf{b} \cdot \nabla)n \right] + \mathcal{D}_{V_{\parallel i}}(V_{\parallel i}) \end{aligned} \quad (4)$$

$$\begin{aligned} \frac{\partial T_e}{\partial t} = & -\frac{R}{\rho_{s0}} \frac{1}{B} [\phi, T_e] - V_{\parallel e}(\mathbf{b} \cdot \nabla)T_e + \frac{4T_e}{3B} \left[ \frac{7}{2} C(T_e) + \frac{T_e}{n} C(n) - C(\phi) \right] \\ & + \frac{2T_e}{3} \left[ 0.71 (\mathbf{b} \cdot \nabla)V_{\parallel i} - 1.71 (\mathbf{b} \cdot \nabla)V_{\parallel e} + 0.71 \frac{(V_{\parallel i} - V_{\parallel e})}{n} (\mathbf{b} \cdot \nabla)n \right] \\ & + \mathcal{D}_{T_e}(T_e) + \mathcal{D}_{T_e}^{\parallel}(T_e) + S_T \end{aligned} \quad (5)$$

which are coupled to Ampère's law,  $\nabla_{\perp}^2 \psi = n(V_{\parallel i} - V_{\parallel e})$ , and to the Poisson equation  $\nabla_{\perp}^2 \phi = \omega$ . We also note that diffusion operators  $\mathcal{D}$  and  $\mathcal{D}^{\parallel}$  have been introduced for numerical purposes: GBS allows the choice between standard diffusion and/or fourth-order hyperdiffusion operators.

The curvature operator,  $C$ , the perpendicular Laplacian operator,  $\nabla_{\perp}^2$ , the parallel gradient,  $\mathbf{b} \cdot \nabla$ , and the Poisson bracket,  $[A, B]$ , that appear in Eqs. (1-5), have to be specified for each geometry; this is made easy by the GBS modular coding. In particular, herein we focus on GBS simulations of turbulence in linear devices, in the SMT geometry, and tokamak SOL.

### 3 Tokamak SOL

Herein we report the first simulations of SOL turbulent dynamics that have been carried out with GBS. We have considered a relatively simple tokamak configuration, with circular flux surfaces, neglecting finite aspect ratio terms and magnetic shear, and with a toroidal limiter located at the equatorial plane, on the high-field side of the machine.

In Fig. 1 we show a snapshot of the plasma pressure. We consider the projections on the poloidal, toroidal, and radial planes. The plasma dynamics that is displayed is the result of the interplay between plasma outflow from the tokamak core, turbulent transport, and losses at the limiter plates, which are located in correspondence of  $y = 0$  and  $y = 800$ . Bohm's boundary conditions are implemented at the limiter plates imposing  $\phi = \Lambda T_e$ .

The plasma outflowing from the core is modeled as density and temperature sources located at  $x = 30$ , uniform in the  $y$  direction and with a gaussian shape in the radial direction, with half width  $w = 5$ . Therefore, the region of interest in the simulation to model the SOL turbulence is for  $x > 30$ . From the source region, plasma is transported in the radial direction by turbulence. In the present SOL simulation, turbulence results from the growth of the resistive ballooning mode that, as displayed by the turbulent snapshots in Figs. 1, has the longest parallel wavelength allowed by the system,  $k_{\parallel} \sim 1/(qR)$ . The poloidal mode number,  $m$ , is constrained between a lower limit, due to the field line bending as for the resistive interchange mode in the SOL, and an upper limit due to curvature-induced plasma compressibility. The toroidal mode number results from  $n \simeq m/q$ . According to the ballooning nature of the instability, turbulence is more active for  $y > 400$ : in fact, it is driven in the unfavorable curvature region on the low-field side of the SOL and then it is convected vertically upwards by the  $\mathbf{E} \times \mathbf{B}$  drift.

Although relatively simple, the present model allows identifying some of the most prominent elements that characterize SOL turbulence measurements. In fact, turbulence presents a coherent dynamics close to the source region while it is dominated in the far SOL by intermittent transport events. Those are the so-called plasma blobs, which have attracted great attention from the plasma physics community since they can be detrimental for the tokamak first wall. Through GBS simulations it is possible to study their dynamics, from their birth to the dissipation on the limiter plates. In general, it is observed that fluctuations have an amplitude comparable to that of equilibrium quantities, and that there is no separation of fluctuation and equilibrium scales. This requires the use of global simulations in order to simulate plasma turbulence, as it is done by GBS.

### 4 Code validation

Validation of plasma turbulence codes plays a fundamental role in assessing maturity of the understanding of plasma dynamics and predictive capabilities of simulations. A validation project is a four step procedure [17, 18]. First (i), the simulation model needs to be qualified; i.e., it is necessary to establish the applicability of the model hypotheses for the simulated physical phenomenon. Second (ii), verification of the code is necessary, in order to prove that the code solves correctly the model equations. Third (iii), simulations

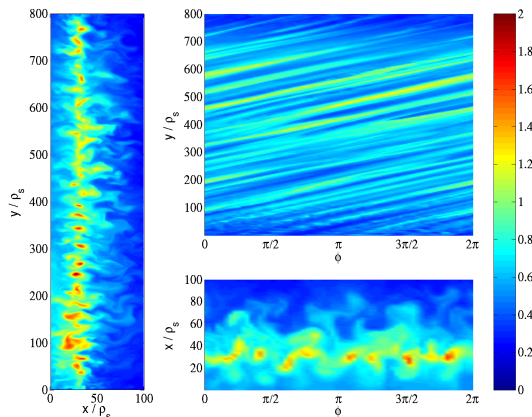


FIG. 1: Snapshot of  $p_e$  in the SOL. A poloidal plane is represented on the left panel, while a radial cut and a toroidal cut are shown on the right upper panel and right lower panel, respectively.

and experiments have to be compared considering a number of physical quantities, common to the experimental measurements and simulation results, and analyzed using the same techniques. These physical quantities, denoted as validation observables, should be identified and organized into a hierarchy. This hierarchy is based on the number of model assumptions and combinations of measurements necessary to obtain the observable; i.e., how stringent each observable is for comparison purposes. Fourth (iv), agreement between simulations and experiments needs to be quantified by using an appropriate composite metric,  $\chi$ . This  $\chi$  coefficient should combine the results of the comparison of all the observables, taking into account position in the hierarchy and precision. Its purpose is to quantify the overall agreement between experiment and simulation. The metric  $\chi$  should be complemented by an index,  $Q$ , which assesses the quality of the comparison. Practically,  $Q$  quantifies the number of observables that have been used for the validation and the strength of the constraints they impose. We remark that the validation procedures should remain simple. The goal is not mathematical rigor, but a useful tool that can be easily applied in order to compare models and assess their predictive capabilities and their limitations.

While model qualification and code verification [point (i) and (ii) of the validation guidelines] are now routinely considered in plasma physics and their methodology has been formulated in considerable detail, only recently has the plasma physics community approached a rigorous methodology for establishing the validation observables and the comparison metric. With the development of the GBS code, we have carried out a validation project with the goal of defining the methodology for the comparison of experimental and simulation results, and we have then applied it to the analysis of the TORPEX device [2, 8].

In Ref. [2], we address point (iii) of the validation methodology. Focusing on observables related to Langmuir probe measurements on TORPEX plasmas, we consider a number of physical quantities that can be used as observables for experiment/simulation

comparison. We classify the observables according to a hierarchy that sums the number of model assumptions and measurement combinations used to obtain an observable from experimental measurements and simulation results. Observables in this hierarchy go from the measurement of the ion saturation current, which is a direct experimental measurement and can be inferred directly from density and temperature simulation data, to the measurement of particle transport, which requires the combination of a number of measurements with hypothesis that also challenge the analysis of simulation data.

The construction of a global metric in order to compare experiments and simulations and the definition of the comparison quality,  $Q$ , point (iv) of the validation methodology, are the subject of Ref. [8]. A key step in the construction of the global metric is the quantification of the agreement between experiment and simulation relative to each observable. We denote with  $e_j$  and  $s_j$  the values of the  $j$ -th observable used in the comparison, as coming from the experimental measurement or the simulation results, respectively. Most of the observables depend on space and time, and typically the value of the observables is given on a discrete number of points, denoted as  $N_j$ . We denote with  $e_{j,i}$  and  $s_{j,i}$  the values of the  $j$ -th observable at points  $i = 1, 2, \dots, N_j$  (the present notation can therefore be used for zero-, one-, two-, etc., dimensional observables). For the  $j$ -th observable, we normalize the distance  $d_j$  between experiments and simulations with respect to the uncertainty related to these quantities:

$$d_j = \sqrt{\frac{1}{N_j} \sum_{i=1}^{N_j} \frac{(e_{j,i} - s_{j,i})^2}{\Delta e_{j,i}^2 + \Delta s_{j,i}^2}}, \quad (6)$$

where  $\Delta e_{j,i}$  and  $\Delta s_{j,i}$  are the uncertainties related to the evaluation of  $e_{j,i}$  and  $s_{j,i}$ . Since simulations and experiments can be considered to agree if they fall within the error bars, we define the level of agreement between experiments and simulations with respect to observable  $j$  as

$$R_j = \frac{\tanh[(d_j - d_0)/\lambda] + 1}{2} \quad (7)$$

with  $R_j \lesssim 0.5$  corresponding to agreement (within the experimental and simulation uncertainties), while  $R_j \gtrsim 0.5$  denoting disagreement (outside the the experimental and simulation uncertainties). Our tests show that the conclusions of a validation exercise are not affected by the specific choices of parameters in the range  $1 \leq d_0 \leq 2$  and  $0.1 \leq \lambda \leq 1$ , therefore the values  $d_0 = 1.5$  and  $\lambda = 0.5$  are reasonable choices.

The overall level of agreement between simulations and experiments can be measured by considering a composite metric, which should take into account the level of agreement of each observable,  $R_j$ , and weight it according to how constraining each observable is for comparison purposes:

$$\chi = \frac{\sum_j R_j H_j S_j}{\sum_j H_j S_j}, \quad (8)$$

where  $H_j$  and  $S_j$  are functions defining the weight of each observable according to its hierarchy level and the precision of the measurement, respectively.

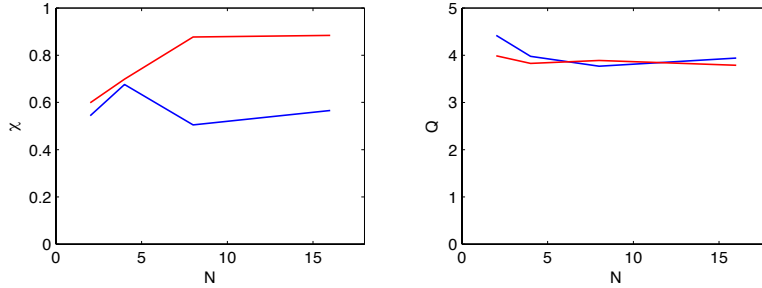


FIG. 2: The results of the GBS validation against TORPEX experimental data are shown. The global metric,  $\chi$ , and the quality of the validation,  $Q$ , is shown for the three-dimensional GBS simulations (blue line) and the two-dimensional one (red line), as a function of  $N$ , the number of field line turns in the SMT.

The definition of  $H_j$  and  $S_j$  is somewhat arbitrary.  $H_j$  should be a decreasing function of hierarchy levels. The definition we adopt is  $H_j = 1/h_j$ , where  $h_j$  is the combined experimental/simulation primacy hierarchy level (see Ref. [2] for more details on the  $h_j$  definition). This definition implies that if no assumptions or combinations of measurements are used for obtaining an observable, then  $H_j = 1$ . The quantity  $S_j$  should be a decreasing function of the experimental and simulation uncertainty. We introduce the following definition:

$$S_j = \exp\left(-\frac{\sum_i \Delta e_{j,i} + \sum_i \Delta s_{j,i}}{\sum_i |e_{j,i}| + \sum_i |s_{j,i}|}\right) \quad (9)$$

such that  $S_j = 1$  in the case of zero uncertainty.

The validation metric should be complemented by an index,  $Q$ , that assesses the "quality" of the comparison. The idea is that a validation is more reliable with a larger number of independent observables, particularly if they occupy a low level in the primacy hierarchy and the measurement and simulation uncertainties are low. The quality of the comparison  $Q$  can thus be defined as

$$Q = \sum_j H_j S_j. \quad (10)$$

We have applied the validation procedure to the study of the TORPEX device. Owing to its detailed diagnostics, possibility of parameter scans, and relatively simple configuration, TORPEX is an ideal testbed to perform experiment/simulation comparisons and to investigate the corresponding methodological framework [12, 13]. As shown in Fig. 2, we perform the comparison between experiments and simulations through a scan in the  $N$  parameter, allowing the properties of the TORPEX turbulence to pass from  $k_{\parallel} = 0$  mode dominated turbulence to  $k_{\parallel} \neq 0$  turbulence. Using a relevant set of observables, we validate two models: a three-dimensional GBS simulations, able to describe the global evolution of TORPEX plasma [6], and the reduced two-dimensional GBS simulations [1], able to describe only the evolution of  $k_{\parallel} = 0$  modes. The validation metric reveals that the agreement of the two-dimensional simulations and the experiment is no longer satisfactory

when  $k_{\parallel} \neq 0$  modes are present in the experiment, which occurs at  $N > 7$ .

We believe that the proposed methodology can be easily applied to discriminate among models, since a smaller  $\chi$  corresponds to a model or a code that provides a better global representation of the physical phenomena at play. Moreover, the proposed methodology is very useful to check how the agreement varies with the control parameters. In fact, the increase of  $\chi$  that follows from a variation of a control parameter points out the presence of a regime where a particular model is not appropriate, presumably because at least one physical phenomenon is not well captured. Thus, the most direct use of the proposed validation methodology is related to determining which code has to be used, and in which parameter regime.

**Acknowledgements.** This work was supported by the Swiss National Science Foundation.

## References

- [1] Ricci P *et al* 2008 *Phys. Rev. Lett.* **100** 225002
- [2] Ricci P *et al* 2009 *Phys. Plasmas* **16** 055703
- [3] Ricci P and Rogers B N 2009 *Phys. Plasmas* **16** 062303
- [4] Ricci P and Rogers B N 2009 *Phys. Plasmas* **16** 092307
- [5] Li B *et al* 2009 *Phys. Plasmas* **16** 082510
- [6] Ricci P and Rogers B N 2010 *Phys. Rev. Lett.* **104** 145001
- [7] Rogers B N and Ricci P 2010 *Phys. Rev. Lett.* **104** 225002
- [8] Ricci P *et al* 2011 *Phys. Plasmas* **18** 032109
- [9] Li B *et al* 2011 *Phys. Rev. E* **5** 056406
- [10] Furno I *et al* 2011 *Plasma Phys. Control. Fusion* **53** 124016
- [11] Gekelman W *et al.* 1991 *Rev. Sci. Instrum.* **62** 2875
- [12] Fasoli A *et al* 2006 *Phys. Plasmas* **13** 055902
- [13] Fasoli A *et al* 2010 *Plasma Phys. Control. Fusion* **52** 124020
- [14] V. Naulin *et al* 1998 *Phys. Rev. Lett.* **81** 4148
- [15] Garcia O E *et al* 2004 *Phys. Rev. Lett.* **92** 165003
- [16] Naulin V and Nielsen A H 2003 *SIAM Journal on Scientific Computing* **25** 104
- [17] Terry P W 2008 *Phys. Plasmas* **15** 062503
- [18] Greenwald M 2010 *Phys. Plasmas* **17** 058101